Received: 2 September 2024 | Revised: 15 October 2024 | Accepted: 4 December 2024 | Published online: 24 December 2024

RESEARCH ARTICLE

Journal of Data Science and Intelligent Systems
2024, Vol. 00(00) 1–8
DOI: 10.47852/bonviewJDSIS42024229

BON VIEW PUBLISHING

The Application of Quantum Pre-Processing Filter for Binary Image Classification with Small Samples

Farina Riaz[1,*], Shahab Abdulla[2], Hajime Suzuki[1], Srinjoy Ganguly[2], Ravinesh C. Deo[3] and Susan Hopkins[3]

[1]*Data61, Commonwealth Scientific and Industrial Research Organisation (CSIRO), Australia*

[2]*UniSQ College, University of Southern Queensland, Australia*

[3]*School of Mathematics, Physics and Computing, University of Southern Queensland, Australia*

Abstract: Over the past few years, there has been significant interest in Quantum Machine Learning (QML) among researchers, as it has the potential to transform the field of machine learning. Several models that exploit the properties of quantum mechanics have been developed for practical applications. In this study, we investigated the application of our previously proposed quantum pre-processing filter (QPF) to binary image classification. We evaluated the QPF on four datasets: MNIST (handwritten digits), EMNIST (handwritten digits and alphabets), CIFAR-10 (photographic images), and GTSRB (real-life traffic sign images). Similar to our previous multi-class classification results, the application of QPF improved the binary image classification accuracy using neural network against MNIST, EMNIST, and CIFAR-10 from 98.9% to 99.2%, 97.8% to 98.3%, and 71.2% to 76.1%, respectively, but degraded it against GTSRB from 93.5% to 92.0%. We then applied QPF in cases using a smaller number of training and testing samples, i.e., 80 and 20 samples per class, respectively. In order to derive statistically stable results, we conducted the experiment with 100 trials choosing randomly different training and testing samples and averaging the results. The result showed that the application of QPF did not improve the image classification accuracy against MNIST and EMNIST but improved it against CIFAR-10 and GTSRB from 65.8% to 67.2% and 90.5% to 91.8%, respectively. Further research will be conducted as part of future work to investigate the potential of QPF to assess the scalability of the proposed approach to larger and complex datasets.

Keywords: quantum machine learning, image classification, quantum circuit, small samples

1. Introduction

Over the past few years, there has been significant interest in Quantum Machine Learning (QML), with various algorithms proposed for image processing [1]. QML has been a hot topic recently [2], especially since quantum hardware development has gradually accelerated [3]. The application of quantum technology in image processing is crucial for efficiently extracting valuable information from real-world scenarios. Numerous approaches have been developed for quantum image classification, such as quantum neural networks [4], quantum convolutional neural network (CNN) [5], hybrid quantum-classical CNN [6], quantum generative adversarial network [7, 8], and quantum support vector machines [9]. The goal of using QML in images is to extract essential features from the image. To achieve this, a classical kernel approach can first be used to estimate unsolvable quantum kernels on a quantum device. Secondly, different models can be created that process the feature vectors using quantum models based on variational circuits. These models gain their strengths by outsourcing nonlinearity into the process of encoding inputs into a quantum state or the quantum feature map. This combination of quantum computing with kernel theory will help in developing QML algorithms that offer potential quantum speedup on near-term quantum devices [10].

Of the various suggested ways to merge classical machine learning techniques with quantum computing [11–18], the method introduced by Henderson et al. in [19] offers several advantages. It can be implemented on quantum circuits with fewer qubits and shallow gate depths, yet it can be applied to more practical use cases. This method employs quantum circuits as transformation layers to extract features for image classification using CNNs. The transformation layers are referred to as quanvolutional layers, and the method is referred as a quanvolutional neural network (QuanvNN) in this research article.

A crucial query arose regarding whether the features generated by quanvolutional layers could enhance the classification accuracy of machine learning models. To investigate this, Henderson et al. have conducted a study where randomly generated quantum circuits were used to compare the classification accuracy of QuanvNN with a standard CNN. However, the findings did not demonstrate a clear advantage in classification accuracy over the classical model [19]. In a subsequent study [20], QuanvNN was updated, implemented on quantum hardware (Rigetti's Aspen-7-25Q-B quantum processing

*Corresponding author: Farina Riaz, Data61, Commonwealth Scientific and Industrial Research Organisation (CSIRO), Australia. Email: farina.riaz@csiro.au

unit), and evaluated on a satellite imagery classification task. Nevertheless, the image classification accuracy of QuanvNN was not improved in comparison to that of a traditional CNN algorithm.

The work of Mari [21] provided an implementation of QuanvNN on a software quantum computing simulator called PennyLane [22]. Their approach differs from that of Henderson et al. [19] in that the output of the quantum circuit, which is a set of expectation values, is directly fed into the subsequent neural network (NN) layer, whereas Henderson et al. [19] transformed it into a single scalar value using a classical method. The proposed method was tested on the MNIST dataset [23], which consists of handwritten digits, using 50 training and 30 test images. However, no clear improvement in classification accuracy by QuanvNN over NN was shown in Mari's study.

In our previous research [24], we extended Mari's QuanvNN by utilizing a randomly generated quantum circuit with four qubits, 20 single-axis rotations, and 10 controlled NOTs (CNOTs) to enhance image classification accuracy when compared to a classical fully connected NN. Specifically, the extended QuanvNN approach improved the accuracy of MNIST and CIFAR-10 datasets (photographic 10 class image dataset [25] from 92.0% to 93.0% and from 30.5% to 34.9%, respectively [24]. We also proposed a new model, NN with quantum entanglement (NNQE), that incorporates a strongly entangled quantum circuit with four qubits, 20 three-axis rotations, 20 CNOTs, and Hadamard gates. This model further increased image classification accuracy against MNIST and CIFAR-10 to 93.8% and 36.0%, respectively [24]. However, using QuanvNN or NNQE was found to degrade the image classification accuracy when applied to a more complicated German Traffic Sign Recognition Benchmark (GTSRB) dataset (43 class real-life traffic sign images [26] in comparison with the classical NN accuracy from 82.2% to 71.9% (QuanvNN) and to 73.4% (NNQE) [24].

The concept of using a quantum circuit as a pre-processing filter for image classification tasks has been extended by the introduction of quantum pre-processing filter (QPF) by Riaz et al. [19]. In Riaz et al. [19], a much-simplified quantum circuit, i.e., a four qubit quantum circuit with Y rotations for encoding and two CNOTs, was introduced. By applying the QPF approach, the results showed that the image classification accuracy based on MNIST and EMNIST (handwritten 47 class digits and letters [28] datasets was improved against classical NN from 92.0% to 95.0% and from 68.9% to 75.8%, respectively. However, tests using the proposed QPF approach against GTSRB showed again a degradation in the classification accuracy from 81.4% to 77.1% [27].

In this study, we first extend the application of QPF using two CNOTs from multi-class classification to binary classification against all possible different pairs of image classes. For 10 classes, e.g., MNIST, the total number of pairs is $10 \times 9 = 90$. For 43 classes, e.g., GTSRB, the total number of pairs is $43 \times 42 = 1{,}806$. The proposed method achieves a higher image classification accuracy of 98.9% compared to 92.5% against MNIST using NN. The image classification accuracy was further improved to 99.2% by the application of QPF. While the image classification against GTSRB was improved from 81.4% to 93.5% using the proposed binary image classification method, the application of QPF degraded the image classification accuracy from 93.5% to 92.0%, similar to our previous results. We note that practical application of the proposed binary classification approach requires an additional categorization method to extract training and testing images corresponding to the chosen classes from larger samples. This additional categorization method is outside of the scope of the current study and is left for further study. In addition, we have applied the two CNOTs QPF to CIFAR-10 and EMNIST datasets and observed the binary image classification accuracy improvements from 71.2% to 76.1% and from 97.8% to 98.3%, respectively.

Secondly, we apply QPF to cases using a smaller number of training and testing samples, i.e., 80 training samples and 20 testing samples per class. The use of a smaller number of samples is considered in application where faster training and testing is required. In order to derive statistically stable results, we conducted the experiment with 100 trials choosing randomly different training and testing samples and averaged the results. The result showed that the application of QPF did not improve the image classification accuracy against MNIST and EMNIST but improved it against CIFAR-10 and GTSRB from 65.8% to 67.2% and from 90.5% to 91.8%, respectively. While the exact cause of this phenomenon is currently under investigation, this result is significant in understanding the effects of QPF in machine learning methods. In order to support our claims, we have made our source codes available at https://github.com/hajimesuzuki999/qpf-bic

The study aims to improve accuracy on a number of image datasets, such as MNIST, GTSRB, CIFAR-10, and EMNIST, by extending the use of the QPF employing two CNOT gates from multi-class to binary classification. The goal of the study is to assess this suggested method's efficacy using a small number of training and testing samples by conducting a quantitative comparison with traditional NN. But there are a few issues that need to be addressed. First, the actual use of the binary classification methodology is complicated since it requires an additional method for classifying training and testing images. Furthermore, the approach has produced variable results across datasets, as the GTSRB dataset shows a decline in accuracy when using the method. Additionally, despite using fewer samples, there have only been slight increases in accuracy, demonstrating performance variability. It is difficult for the experimental design to produce statistically stable results when sample sizes are small. Furthermore, in certain scenarios, the challenges involved in implementing QPF may make it impractical. The different ways of QPF affect accuracy points different, for different datasets leads to further investigation to better understand its underlaying mechanisms to further develop how it can be applied to different applications.

The structure of this research paper is as follows: Section 2 outlines the methodology of our proposed model. Section 3 provides a detailed account of our experimental setup. Section 4 contains the results and discussion. Finally, in Section 5, we present our conclusions.

2. Methodology

The architecture of QPF was first proposed in Riaz et al. [27]. For the sake of completeness, we reproduce the description of QPF in this section. Figure 1 shows the architecture of the proposed QPF.

2.1. Input image preparation

The method assumes that the input image is a two-dimensional matrix with size m-by-m, and the pixel value x, follows $0 \leq x \leq 1$. An extension to a multi-channel pixel image is considered as straightforward.

Figure 1
The architecture of the QPF model

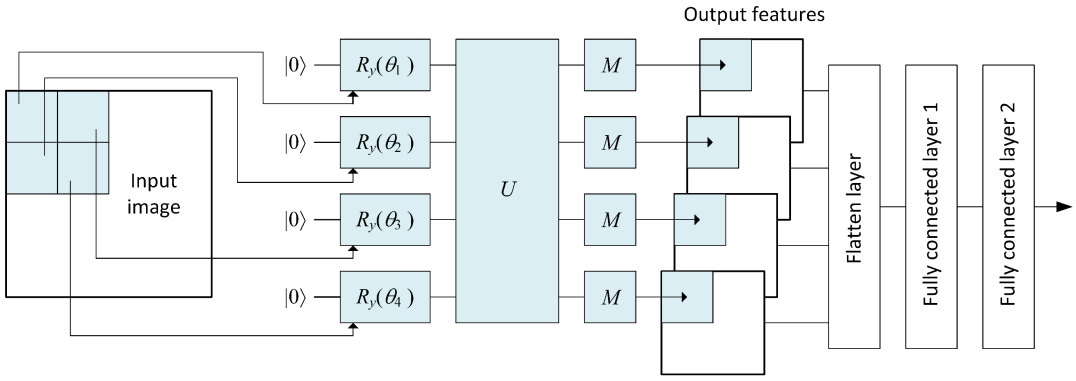

2.2. RY gate encoding

The RY gate is used to encode each pixel value into a quantum state in order to get the image ready for quantum processing. The RY gate is a quantum gate that rotates the Bloch sphere by a certain angle θ around its Y-axis. The rotation angle θ in this case is determined as $\theta = 2\pi x$, which is proportional to the pixel intensity x. By rotating the pixel intensity, the classical state becomes a quantum state, which opens up the possibility of performing further quantum computations on the image data.

2.3. QPF window extraction

The input image is processed to extract a portion of size n-by-n, where n is the window size that the QPF model uses. The suggested QPF approach selects a 2×2 portion of the input image, called the QPF window, with $n = 2$. After that, the quantum circuit processes and encodes this little portion. Depending on the pixel intensity, the RY gate rotates qubits by an angle $\theta = 2\pi x$ when applied to each pixel value within the window. After that, the encoded data are subjected to quantum operations via the QPF model, which preserves the controllable quantum circuit complexity while extracting localized features.

2.4. Quantum circuit implementation

The outputs from the Y rotation gates are fed to the quantum circuit referred as *U* in Figure 1. The structure of this circuit, as detailed in Figure 2, includes two CNOT gates configured to exploit quantum entanglement properties. The specific arrangement used was determined from previous experiments, ensuring optimal performance.

2.5. Measurement operations

Measurements, referred as *M* in Figure 1, are performed on the output of the quantum circuit *U*. The structure of the quantum circuit *U* is further detailed in Figure 2. In Riaz et al. [27], we conducted experiments with different CNOT arrangement (quantum entanglement property of quantum mechanics) and found that the arrangement as given in Figure 2 showed superior improvements in image classification accuracy. The outputs from the measurement operations are given as expectation values between −1 and 1, and form output features. We note that the total number of parameters in the input image ($m \times m$) is the same as the total number of parameters in the output features ($4 \times (m/2) \times (m/2)$).

Figure 2
QPF with two CNOTs

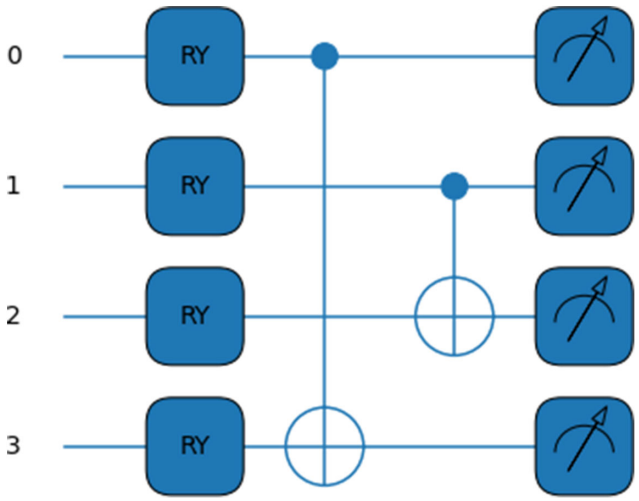

2.6. Feature flattening and connection layers

The output features are made into a one-dimensional vector by the fatten layer. The number of nodes of the output of the flattening layer is $m \times m$. The nodes are fully connected by the first fully connected layer 1. The output of the fully connected layer 2 has the number of nodes equal to the number of classes.

The experimental methodology included multiple tests, with each combination examined over 100 random iterations to ensure the reliability and validity of the results. Because training and testing samples were chosen separately during these experiments, statistically stable results could be obtained. This randomization ensures that the findings from the experiments are robust and applicable to a larger range of applications while also reducing potential biases and strengthening the findings' generalization.

Next section will show the details of Experimental setup and the materials used for the proposed methodology.

3. Experiment

The Quantum Penny-lane Simulator (Python) and MATLAB programming languages have both been used in the implementation of the proposed approach. Because of its strong mathematical and numerical processing skills, MATLAB is usually recommended for activities like algorithm building, data analysis, and visualization. By comparison, Python is renowned for its rich libraries and versatility, which make scientific computing, data manipulation, and machine learning easier. MATLAB's powerful computational tools and Python's vast ecosystem of libraries and frameworks are used in this implementation to maximize the overall efficacy and efficiency of the proposed strategy. Better integration of diverse capabilities and ease of use throughout different phases of the implementation process are also made possible by this dual-language approach. The Adam optimizer and a batch size of 128 have been used for training the network. Four datasets were utilized: MNIST, EMNIST, CIFAR-10, and GTSRB.

The MNIST dataset comprises of 60,000 training and 10,000 testing images of handwritten digits ranging from 0 to 9 [23]. Each image is of size 28 by 28 pixels. The original images are represented in grayscale with pixel values between 0 and 255, which are normalized by dividing them by 255. Figure 3 shows some examples of images from the MNIST dataset.

The EMNIST dataset comprises 112,800 training and 18,800 test images of handwritten digits and letters making up 47 classes [28]. The image size and scaling are the same as MNIST dataset. The CIFAR-10 dataset comprises 50,000 training and 10,000 test images of 10 class photographic images [25]. The original images are in RGB color, which were converted into grayscale between 0 and 255 and then scaled by dividing them by 255.

The GTSRB dataset [26] comprises 34,799 training and 12,630 test images of 43 different classes of traffic signs. These images are actual pictures of traffic signs captured under different conditions. The size of the original images varies between 15 × 15 and 222 × 193 pixels. However, in this experiment, all images have been scaled to a size of 32 × 32 pixels. The images in the dataset are initially in RGB color format, but they were converted into grayscale, with pixel values ranging between 0 and 255. Then, the pixel values were scaled down by dividing them by 255 to normalize the data. Figure 4 provides some examples of images from the GTSRB dataset.

Table 1 summarizes the parameters of the three image datasets used in the experiment.

Figure 3
Example MNIST dataset images

Figure 4
Example GTSRB dataset images

Table 1
Parameters of image datasets used in the experiment

	MNIST	EMNIST	CIFAR-10	GTSRB
Image size	28 × 28	28 × 28	32 × 32	32 × 32
No of color channel	1	1	3	3
No of classes	10	47	10	43
No of class pairs	90	2,162	90	1,806

4. Results and Discussion

First, we use all available training and testing samples to perform binary image classification against all different pairs of classes using NN. The results are shown in Figure 5(a) for MNIST dataset. In this graph, the testing accuracy for the given pair is shown by a different color. For example, classifying the number 0 against 1 achieves close to 100% accuracy, as shown in light yellow. In comparison, we can observe that the testing accuracy for number 5 against 8 is poor, about 96% accuracy. This is due to the similarity in the shapes of the handwritten numbers 5 and 8. Additionally, other class pairs such as 3 and 5, 3 and 8, 4 and 9, and 7 and 9 also have similar shapes, leading to lower testing accuracy for those pairs. On average, the binary image classification using classical NN against MNIST achieved 98.9% testing accuracy using all data.

In the current investigation, we visually represent the classification performance across several datasets and experimental settings using a color-coded accuracy heatmap to display the results. The heatmap's squares each reflect an accuracy number, and the color gradient offers a clear explanation of the findings. The color scale runs from yellow to purple, with yellow indicating the highest accuracy value (almost 100%) and darker hues denoting decreasing accuracy values as they transition towards purple. An accurate comparison of accuracy levels is made possible by this visualization method, which effectively displays the performance variances across different class pairs and trials.

Figure 5(b) shows the results for QPF-NN against MNIST using all data. A similar result is obtained with 99.2%. When it is applied to EMNIST and CIFAR-10, QPF-NN improved the testing accuracy over NN from 97.8% to 98.3% and from 71.2% to 76.1%, respectively.

Figure 6(a) shows the NN results against GTSRB using all data. We can identify pairs of classes that produce high testing accuracy and those that do not. For example, class 7 shows lower testing accuracy against many of the classes between 20 and 43, compared to class 6 or 8, as indicated by the red oval. Referring to Stallkamp et al. [26], Figure 1, class 7 corresponds to 80 km/h sign with a diagonal strip. This class also has a smaller number of samples (Approx. 1/3) compared to class 6 or 8. Detailed examination of this graph may provide further insights; however,

Figure 5
Testing accuracy against MNIST using all data. (a) Using NN (b) Using QPF-NN

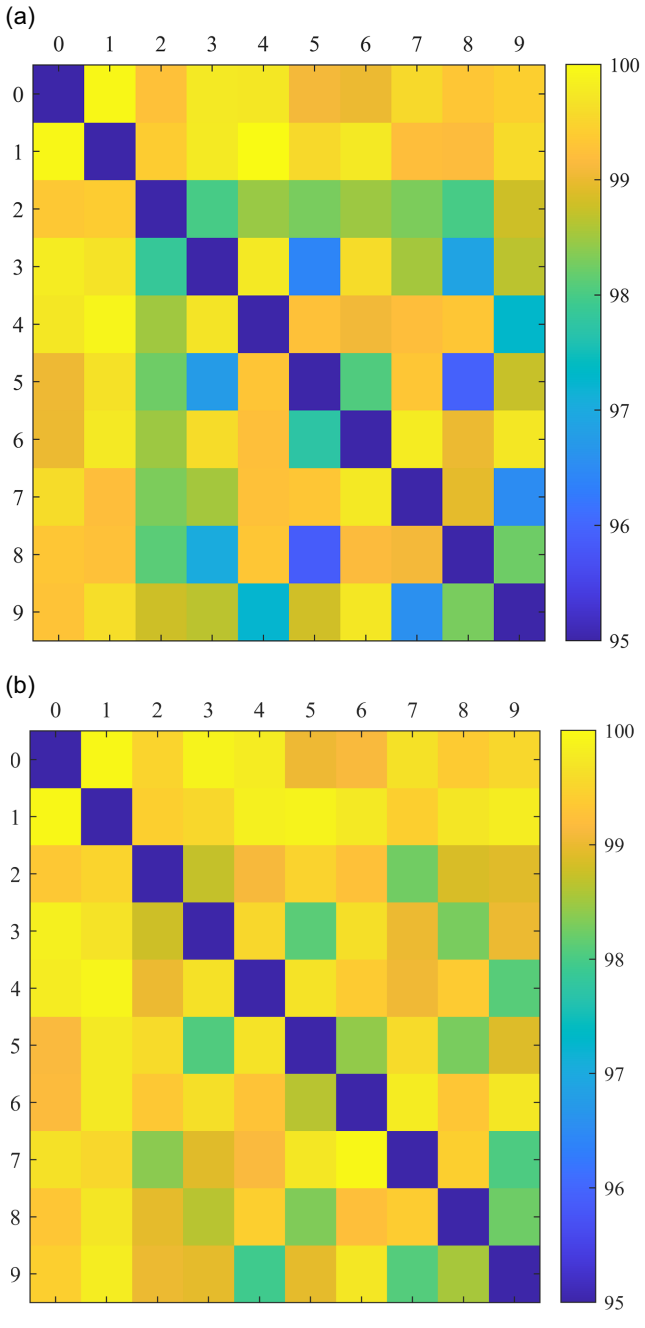

Figure 6
Testing accuracy against GTSRB using all data. (a) Using NN (b) Using QPF-NN

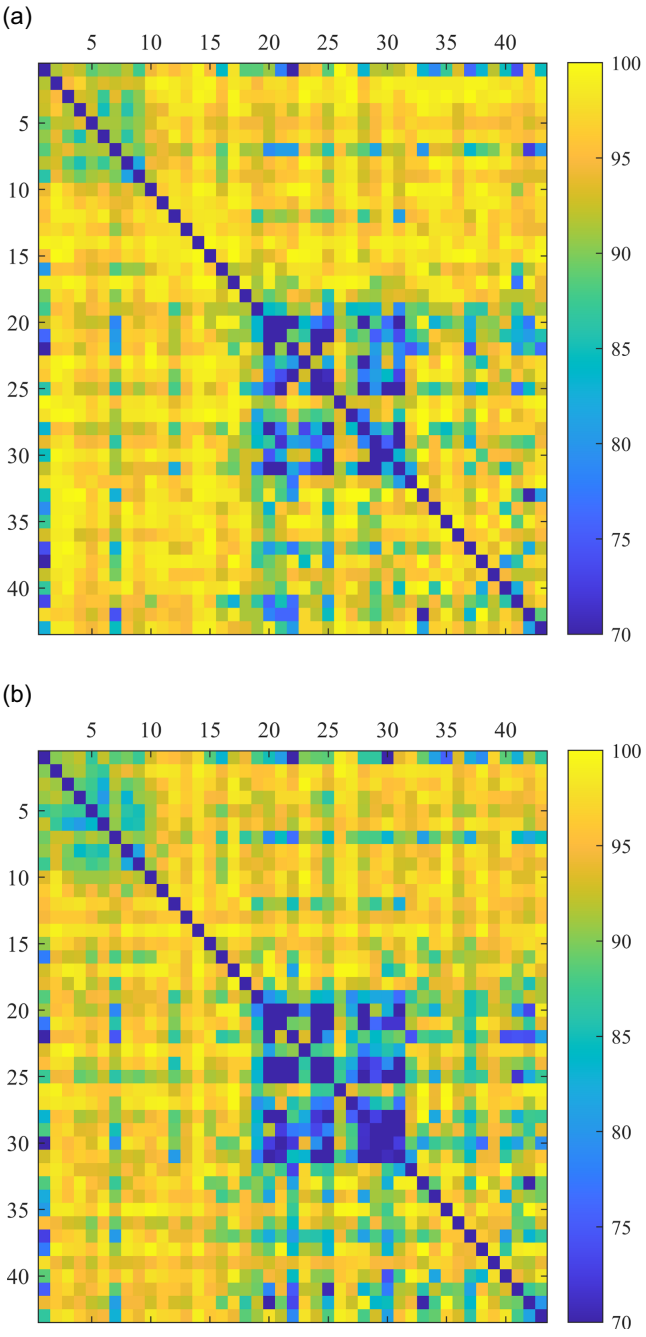

we focus on the effects of the application of QPF, and hence, this is left for a future study. The average testing accuracy over all different pairs is 93.5%. In comparison, Figure 6(b) shows the QPF-NN results against GTSRB using all data. Similar results were obtained with a reduced average testing accuracy of 92.0%.

Secondly, we performed 100 trials with each trial extracting 80 training samples and 20 testing samples per class randomly to perform training and testing. Figure 7 shows the variation of testing accuracy as a function of a trial index when NN and QPF-NN are used against MNIST. We observe that variation is relatively large (approximately 3%) which shows the importance of performing multiple trials and averaging the results to obtain statistically stable results. On average, the testing accuracy of 94.7% and 94.5% was obtained for NN and QPF-NN, respectively. In this case, the application of QPF shows minimal effects. Similarly, we observed minimal effects of using QPF-NN over NN against EMNIST having the same testing accuracy of 94.0%.

Figure 8 shows the results against GTSRB. We observe that the variation is relatively small (approximately 1%) which may be due to a larger number of class pairs (1,806 for GTSRB compared to 90 for MNIST) over which the testing accuracy is averaged for each trial. Importantly, the application of QPF shows improvement over NN against GTSRB, which was not observed in any of our previous experiments.

Figure 7
Testing accuracy against MNIST using 100 samples and 100 trials

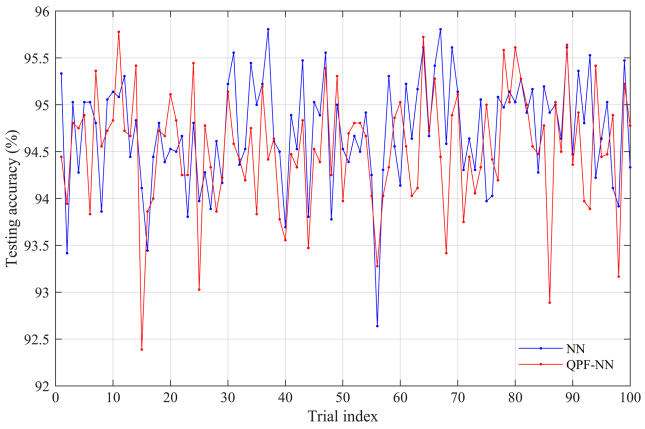

Figure 8
Testing accuracy against GTSRB using 100 samples and 100 trials

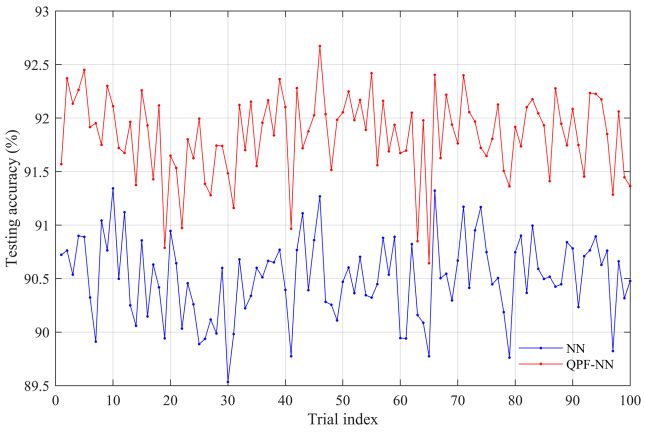

It is also notable that QPF-NN always improved the testing accuracy over NN in any of the 100 trials. We note that the same set of training and testing samples was used for NN and QPF-NN for each trial. We have observed a similar result with CIFAR-10 with an improved test accuracy from 65.8% to 67.2%. A summary of the testing accuracy results is shown in Table 2.

Table 2
A summary of testing accuracy results

	MNIST	EMNIST	CIFAR-10	GTSRB
All data, NN	98.9%	97.8%	71.2%	93.5%
All data, QPF-NN	99.2%	98.3%	76.1%	92.0%
100 samples, NN	94.7%	94.0%	65.8%	90.5%
100 samples, QPF-NN	94.5%	94.0%	67.2%	91.8%

5. Conclusion

This study aimed to evaluate the performance of a proposed binary image classification method using a QPF model with 4 qubits and 2 CNOTs. In our previous research [27], we have shown that QPF is used for efficient image feature extraction while existing quantum circuits demand high computation and multiple layers to extract image features. Similar to the previously reported multi-class classification case, the proposed QPF model improved binary image classification accuracy against MNIST, EMNIST, and CIFAR-10 but we observed a slight decrease in the performance against GTSRB using all training and testing samples. The GTSRB dataset, which has more complex features and a wider variety of visual representations than the other datasets, may be the cause of this decline in accuracy due to its complexity and variability. Subtle variations in shape, color, and orientation are common in traffic sign images, which makes it harder for the QPF model to be generalized across all classes. In spite of this, the outcomes demonstrate the advantages of QPF, especially with regard to reduced computing costs. These results offer useful insights for optimizing quantum-based image classification techniques and focusing future research to improve performance on increasingly challenging datasets such as GTSRB.

However, when applied to the cases with a smaller number of training and testing samples, QPF improved image classification performance against CIFAR-10 and GTSRB, which shows better generalization of our QPF model for smaller number of samples compared to previous classical NN models, which mostly requires a larger number of sample to generalize [29]. The results presented in this article provide further insights into the effects of QPF on machine learning algorithms. QPF has a clear advantage over conventional approaches because of its capacity to generalize with fewer samples, which implies its potential value in situations where gathering huge amounts of labeled data is difficult. However, there is still much to learn about QPF's scalability to larger and more complicated datasets. Even though CIFAR-10 and GTSRB are diverse datasets, their complexity is still lower than that of the larger datasets that are frequently utilized in real-world applications, where there is a significant increase in quantity of data, image diversity, and feature complexity. In order for QPF to process and generalize from a wider variety of features and samples, its quantum architecture will need to be modified in order to scale it to handle such datasets. The preliminary discussion may center on hybrid quantum-classical methods, quantum resource optimization (gate depth, qubit numbers, etc.,), or creating methods for effectively handling larger data sets in the QPF framework. When the model is used in larger use cases, practical issues like processing requirements and the effect of quantum noise will also need to be taken into account. In order to determine whether QPF can scale well and continue to be a practical option for challenging, real-world machine learning problems, future research will examine these challenges. Furthermore, more mechanistic analysis and sufficient dataset validation remain required to determine whether QPF is generalizable for multi-target classification of small-sample images, but it is certainly a worthwhile and fascinating area of exploration.

Acknowledgement

This research has been supported by Australian Government Research Training Program and Commonwealth Scientific Industrial and Research Organization.

Ethical Statement

This study does not contain any studies with human or animal subjects performed by any of the authors.

Conflicts of Interest

The authors declare that they have no conflicts of interest to this work.

Data Availability Statement

The data that support the findings of this study are openly available in GitHub at https://github.com/hajimesuzuki999/qpf-bic.

Author Contribution Statement

Farina Riaz: Conceptualization, Methodology, Software, Validation, Formal analysis, Investigation, Resources, Data curation, Writing – original draft, Writing – review & editing, Visualization, Project administration. **Sharhab Abudlla:** Validation, Formal analysis, Investigation, Resources, Data curation, Writing – original draft, Writing – review & editing, Supervision. **Hajime Suzuki:** Methodology, Validation, Formal analysis, Investigation, Resources, Data curation, Writing – original draft, Writing – review & editing, Visualization, Supervision, Project administration. **Srinjoy Ganguly:** Conceptualization, Methodology, Software, Validation, Formal analysis, Investigation, Resources, Data curation, Writing – original draft, Writing – review & editing, Visualization, Supervision, Project administration. **Ravinesh C. Deo:** Investigation, Resources, Data curation, Writing – review & editing, Supervision. **Susan Hopkins:** Writing – review & editing, Supervision.

References

[1] Cerezo, M., Verdon, G., Huang, H. Y., Cincio, L., & Coles, P. J. (2022). Challenges and opportunities in quantum machine learning. *Nature Computational Science*, *2*(9), 567–576.

[2] Huang, H. L., Xu, X. Y., Guo, C., Tian, G., Wei, S. J., Sun, X., … , & Long, G. L. (2023). Near-term quantum computing techniques: Variational quantum algorithms, error mitigation, circuit compilation, benchmarking and classical simulation. *Science China Physics, Mechanics & Astronomy*, *66*(5), 250302.

[3] Clarke, J., & Wilhelm, F. K. (2008). Superconducting quantum bits. *Nature*, *453*(7198), 1031–1042.

[4] Cerezo, M., Arrasmith, A., Babbush, R., Benjamin, S. C., Endo, S., Fujii, K., … , & Coles, P. J. (2021). Variational quantum algorithms. *Nature Reviews Physics*, *3*(9), 625–644.

[5] Cong, I., Choi, S., & Lukin, M. D. (2019). Quantum convolutional neural networks. *Nature Physics*, *15*(12), 1273–1278.

[6] Liu, J., Lim, K. H., Wood, K. L., Huang, W., Guo, C., & Huang, H. L. (2021). Hybrid quantum-classical convolutional neural networks. *Science China Physics, Mechanics & Astronomy*, *64*(9), 290311.

[7] Lloyd, S., & Weedbrook, C. (2018). Quantum generative adversarial learning. *Physical Review Letters*, *121*(4), 040502.

[8] Huang, H. L., Du, Y., Gong, M., Zhao, Y., Wu, Y., Wang, C., … , & Pan, J. W. (2021). Experimental quantum generative adversarial networks for image generation. *Physical Review Applied*, *16*(2), 024051.

[9] Havlíček, V., Córcoles, A. D., Temme, K., Harrow, A. W., Kandala, A., Chow, J. M., & Gambetta, J. M. (2019). Supervised learning with quantum-enhanced feature spaces. *Nature*, *567*(7747), 209–212.

[10] Schuld, M., & Killoran, N. (2019). Quantum machine learning in feature Hilbert spaces. *Physical Review Letters*, *122*(4), 040504.

[11] Li, Y., Liu, R., Hao, X., Shang, R., Zhao, P., & Jiao, L. (2023). EQNAS: Evolutionary quantum neural architecture search for image classification. *Neural Networks*, *168*, 471–483.

[12] Abdel-Khalek, S., Algarni, M., Mansour, R. F., Gupta, D., & Ilayaraja, M. (2023). Quantum neural network-based multi-label image classification in high-resolution unmanned aerial vehicle imagery. *Soft Computing*, *27*, 13027–13038.

[13] Chen, G., Chen, Q., Long, S., Zhu, W., Yuan, Z., & Wu, Y. (2023). Quantum convolutional neural network for image classification. *Pattern Analysis and Applications*, *26*(2), 655–667.

[14] Bai, Q., & Hu, X. (2023). Quantity study on a novel quantum neural network with alternately controlled gates for binary image classification. *Quantum Information Processing*, *22*(5), 184.

[15] Wang, A., Hu, J., Zhang, S., & Li, L. (2024). Shallow hybrid quantum-classical convolutional neural network model for image classification. *Quantum Information Processing*, *23*(1), 17.

[16] Wu, S., Li, R., Song, Y., Qin, S., Wen, Q., & Gao, F. (2024). Quantum assisted hierarchical fuzzy neural network for image classification. *IEEE Transactions on Fuzzy Systems*, 1–12.

[17] Shi, M., Situ, H., & Zhang, C. (2024). Hybrid quantum neural network structures for image multi-classification. *Physica Scripta*, *99*(5), 056012.

[18] Senokosov, A., Sedykh, A., Sagingalieva, A., Kyriacou, B., & Melnikov, A. (2024). Quantum machine learning for image classification. *Machine Learning: Science and Technology*, *5*(1), 015040.

[19] Henderson, M., Shakya, S., Pradhan, S., & Cook, T. (2020). Quanvolutional neural networks: Powering image recognition with quantum circuits. *Quantum Machine Intelligence*, *2*(1), 2.

[20] Henderson, M., Gallina, J., & Brett, M. (2021). Methods for accelerating geospatial data processing using quantum computers. *Quantum Machine Intelligence*, *3*(1), 4.

[21] Mari, A. (2024). *Quanvolutional neural network.* Retrieved from: https://pennylane.ai/qml/demos/tutorial_quanvolution

[22] Bergholm, V., Izaac, J., Schuld, M., Gogolin, C., Ahmed, S., Ajith, V., … , & Killoran, N. (2018). Pennylane: Automatic differentiation of hybrid quantum-classical computations. *arXiv Preprint:1811.04968*.

[23] LeCun, Y., Bottou, L., Bengio, Y., & Haffner, P. (1998). Gradient-based learning applied to document recognition. *Proceedings of the IEEE*, *86*(11), 2278–2324.

[24] Riaz, F., Abdulla, S., Suzuki, H., Ganguly, S., Deo, R. C., & Hopkins, S. (2023). Accurate image multi-class classification neural network model with quantum entanglement approach. *Sensors*, *23*(5), 2753.

[25] Krizhevsky, A., & Hinton, G. (2009). *Learning multiple layers of features from tiny images*. Master's Thesis, University of Toronto.

[26] Stallkamp, J., Schlipsing, M., Salmen, J., & Igel, C. (2011). The German traffic sign recognition benchmark: A multi-class classification competition. In *The 2011 International Joint Conference on Neural Networks*, 1453–1460.

[27] Riaz, F., Abdulla, S., Suzuki, H., Ganguly, S., Deo, R. C., & Hopkins, S. (2023). Development of a novel quantum

pre-processing filter to improve image classification accuracy of neural network models. *arXiv Preprint: 2308.11112*.

[28] Cohen, G., Afshar, S., Tapson, J., & van Schaik, A. (2017). EMNIST: Extending MNIST to handwritten letters. In *2017 International Joint Conference on Neural Networks*, 2921–2926.

[29] Caro, M. C., Huang, H. Y., Cerezo, M., Sharma, K., Sornborger, A., Cincio, L., & Coles, P. J. (2022). Generalization in quantum machine learning from few training data. *Nature Communications*, *13*(1), 4919.

How to Cite: Riaz, F., Abdulla, S., Suzuki, H., Ganguly, S., Deo, R. C., & Hopkins, S. (2024). The Application of Quantum Pre-Processing Filter for Binary Image Classification with Small Samples. *Journal of Data Science and Intelligent Systems*. https://doi.org/10.47852/bonviewJDSIS42024229